Research article

Spatial distribution, patterns and source contributions of POPs in the atmosphere of Great Mendoza using the WRF/CALMET/CALPUFF modelling system

M.F. Ruggeri [a, b, c], N.B. Lana [d, e], J.C. Altamirano [a, e], S.E. Puliafito [b, f, *]

[a] Laboratorio de Química Ambiental, Instituto Argentino de Nivología, Glaciología y Ciencias Ambientales (IANIGLA, CCT-CONICET), P.O. Box 131, Mendoza, 5500, Argentina
[b] Universidad Tecnológica Nacional, Facultad Regional Mendoza, Rodriguez 273, Mendoza, Argentina
[c] Centro de Tecnologías Ambientales, Universidad Técnica Federico Santa María, Valparaíso, Chile
[d] Instituto Argentino de Nivología, Glaciología y Ciencias Ambientales (IANIGLA, CCT-CONICET), Argentina
[e] Facultad de Ciencias Exactas y Naturales, Universidad Nacional de Cuyo, Mendoza, Argentina
[f] Consejo Nacional de Investigaciones Científicas y Técnicas (CONICET), Argentina

ARTICLE INFO

ABSTRACT

Global monitoring of Persistent Organic Pollutants (POPs) has allowed the knowledge of levels and distribution around the world as well as the understanding of its transport through the atmosphere. However, there are still some gaps in this regard, especially in some locations, as the case of Great Mendoza, a medium-sized urban area located in the center-west of Argentina. In this work, the WRF/CALMET/CALPUFF modeling system was used to estimate airborne levels of four families of POPs (PCBs, PBDEs, DDTs and HCB) in the study area. The model was validated from measured data obtained from eleven sites using passive air samplers with polyurethane foam disks (PUFs), subsequently analyzed by GC-ECNI/MS. Considering both sets of data, measured and simulated airborne concentrations, five statistical performance metrics were calculated for each family of POP [Mean bias error, (MBE), Fractional Bias (FB), Normalized Mean Square Error (NMSE), Factor of two (Fa2) and Pearson correlation coefficient (r)]. Results exhibited a good agreement between modeled and measured data, showing that WRF/CALMET/CALPUFF modeling system predicts POPs airborne concentrations with reasonable accuracy at a local scale. Model output was used to examine the relative source contribution to ground-level concentrations and to assess the spatial variability of the studied POPs in the study area. Source apportionment showed the prevalence of emissions from open burning of municipal solid waste (ranging from 9% to 90%) on the simulated atmospheric concentrations. HCB presented the lowest mean contribution from this activity (37%) but the highest variability (SD = 20%), followed by PCBs (69 ± 9%), and PBDEs (84 ± 4%). The spatial pattern obtained from simulations exhibited that both, lowest and highest levels predicted by the model, occurred in areas where no samples were taken, suggesting that the real gradient in the POPs air concentrations would be much greater than those reflected by measured data. This work highlights the usefulness of the implementation of an atmospheric dispersion model, not only in the study of air quality and exposure levels but also as a tool for the proper design of monitoring networks, taking into account the time and cost that sampling campaigns take, and the conclusions that are intended to be made from the analysis of the obtained data.

1. Introduction

Persistent organic pollutants (POPs) are characterized by their persistence in the environment, ability to bioaccumulate and biomagnify in ecosystems, susceptibility to long-range atmospheric transport as well as their significant adverse effects on human

* Corresponding author. Universidad Tecnológica Nacional, Facultad Regional Mendoza, Rodriguez 273, Mendoza, Argentina.
E-mail address: epuliafito@frm.utn.edu.ar (S.E. Puliafito).

health and the environment [1]. International efforts have been made to reduce levels and emissions of POPs, including the Stockholm Convention, an international treaty signed in 2001 and came into force in 2004. The Convention considers a wide range of substances such as organochlorine pesticides; industrial chemicals and unintentional byproducts, mainly from combustion activities [1].

Like other 31 Countries and States from Latin American and the Caribbean [2], Argentina adhered to the Convention in 2005 [3]. With the objective of fulfilling this assumed commitment, some actions have been carried out in Argentina, even before that date. The related legislation was gradually updated, in order to ban the manufacture, importation and use of this type of substances, mainly organochlorine pesticides (OCPs) [4], and polychlorinated biphenyls (PCBs) [5]. Likewise, there are still some POPs that have not been regulated, such as polybrominated diphenyl ethers (PBDEs), used mainly as flame retardants (FRs), which are still unrestricted in the country. Beyond the regulatory efforts, certain anthropogenic activities are not regulated and emit POPs to the environment. In the case of OCPs, some current-use pesticides include dichloro-diphenyl-trichloroethane (DDT) and hexachlorobenzene (HCB) in their formulations, either as precursors (dicofol that emits DDT) or as a minor part of the active ingredients (PCNB and chlorothalonil that emit HCB) [6]. Regarding PCBs, they were widely used in electrical transformers until they were regulated by the Argentine law 25.670 from 2002, which aimed that by 2010 none installed equipment should remain in the entire territory of the Nation containing PCBs [5]. However, the elimination or decontamination of these equipment has been gradual, leading to the presence of point-sources.

Furthermore, some urban and industrial activities are associated with POPs releases into the environment. Unintentional emissions caused by open burning events or incineration of products containing chlorinated or brominated compounds constitute a significant atmospheric source of PCBs, HCB and PBDEs, as well as dioxins [6,7]. Likewise, the addition of FRs to consumer goods polymers represents a well-known source of emission of PBDEs into the atmosphere [6].

Additionally to the legislation update, some studies aimed at generating data about environmental levels and releases of POPs in the country have been conducted. However, these studies are scarce and there are still some gaps in this respect [6,8], with limited information on air concentrations of POPs in Argentina. Previous works have determined airborne levels of OCPs and PCBs [7–10], with fewer reports about concentrations of PBDEs and HCB [10–13]. These studies, like many others around the world [10,13–18], used polyurethane foam disk passive samplers (PUFs) to sampling and determining atmospheric concentrations of POPs. These samplers are characterized by their high retention rate, low cost and simple handling [19]. The data generated by them can help to develop and test emissions estimates and can be used to validate predictions from fate and transport models [20].

However, it is well known that the information achieved when using PUFs, has limitations regarding the representativeness of the taken samples due to the low temporal resolution and unknown spatial resolution. These limitations must be considered to ensure the validity of the data obtained and the conclusions drawn from them [21]. The use of a dispersion model based on an emissions inventory emerges as a complement of the analytical determinations, to obtain greater spatial and temporal representativeness. By using this type of model, a relationship between anthropogenic activities that produce the emissions and the levels of POPs in the environment can be established. Among the wide variety of models currently available, CALPUFF (California Puff) model presents a superior capacity to estimate dispersion in complex environments. The Guide on Air Quality Models of the United States Environmental Protection Agency [22] recommends its use over other regulatory models for applications where the terrain contains variations in the relief and where land cover is not uniform.

This work aimed to comprehensively evaluate atmospheric POPs patterns and their spatial variability over Great Mendoza, a medium-sized city in central-western of Argentina, characterized by the combination of an urban nucleus with high population density (about 1 million inhabitants in 2010) with rural peripheries of intensive agricultural activity in the foothills of the Andes Mountain Range. Determinations of atmospheric concentrations of four POPs (DDTs, HCB, PCBs, PBDEs) using PUFs in eleven sites of the study area are presented. Furthermore, the atmospheric dispersion of selected POPs was simulated using the WRF/CALMET/CALPUFF modeling system [23,24], based on a high-resolution emission inventory previously elaborated by the authors, for the same compounds determined analytically in the PUFs [6]. The implemented model also served as a tool to evaluate the emission inventory mentioned above.

The combination of both, determinations of atmospheric levels of POPs and the operation and validation of the dispersion model, constitutes the first study of its type in the study area, so this work represents an important contribution to the knowledge and preservation of the air quality and public health. Furthermore, this work addressed the gap in data and delivered base information about POPs levels in the air in Great Mendoza. It will also serve as a baseline against which future concentrations in the air can be compared and as a tool for the proper design of monitoring networks, taking into account the time and cost that sampling campaigns take, and the conclusions that are intended to be made from the analysis of the obtained data.

2. Materials and methods

2.1. Study area

Great Mendoza (Fig. 1) is the most important urban area in Western Argentina and the fourth in population of the country (about 1 million inhabitants in the last census from 2010). The conurbation is located in the west-central part of the country, in a region of foothills and high plains, on the eastern side of the Andes, between 32° and 37° 35′ S, and 66° 30′ and 70° 35′ W. The urbanized area, about 16700 km^2, extends in an irregular way to the
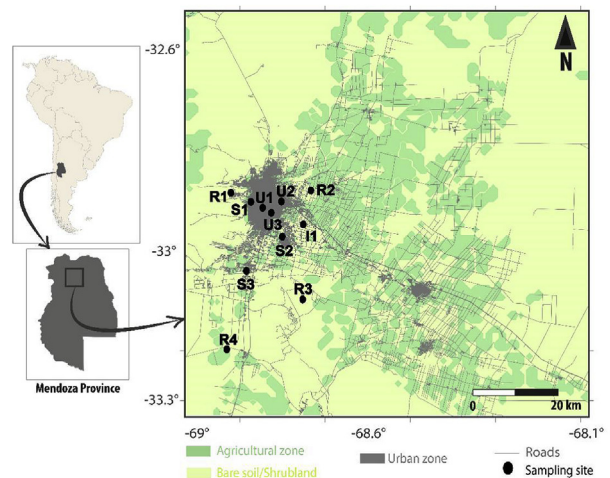

Fig. 1. Great Mendoza study area with land use features and location of sampling sites. U: Urban sites, S: Suburban sites, R: Rural sites.

northeast, east and south, since the Andes Range prevents the growth of the city to the west. The surrounding area is a productive river oasis and the most important wine region in the country, accounting for nearly two-thirds of the country's wine production. Other important crops are apples, pears, tomatoes, onions, plums, olives, cherries, peaches and quince. Major industrial complexes are located in two areas in the periphery of the city to the SW and the north edge, while the agricultural and food production is mostly located on the south and east sides. Minor manufacturing facilities are dispersed in small industrial districts near the urban center. Several active urban waste disposal sites are situated in the periphery or integrated into suburban areas [6].

From the climatic point of view, Great Mendoza is located in a semiarid region, with low relative humidity (<50%), very low precipitation rates (230 mm yr^{-1}) and marked seasonality, with precipitation mainly occurring during Austral summer months. The closeness of the Andes Mountains has a strong influence on local meteorology and air quality, characterized by a day-night variation due to a typical valley-mountain circulation [25].

2.2. Air sampling and analysis

The compounds targeted in this study are: 36 PCB congeners (IUPAC no: 18, 28, 31, 44, 47, 49, 52, 66, 74, 87, 95, 99, 101, 105, 110, 118, 128, 132, 138, 146, 149, 151, 153, 156, 170, 171, 174, 177, 180, 183, 187, 194, 195, 199, 206, 209); 8 PBDE congeners (no: 28, 47, 99, 100, 153, 154, 183, 209), 2 DDT isomers (o,p′-DDT and p,p′-DDT), and hexachlorobenzene (HCB).

Although the determination and quantification of PCBs and PBDEs were carried out differentiating by congener and DDT by isomer, the report of the results, as well as the dispersion modeling were done in sum basis.

2.2.1. Sample collection

Passive air samplers with polyurethane foam disks (14 cm diameter x 1.2 cm thickness; surface area 365 cm^2, volume 207 cm^3 and density 0.021 g cm^{-3}, Tisch Environmental, USA) [26] were used to collect air samples during the period from December 2010 to April 2011 (Austral summer) at 11 sites in the study area. The filters were deployed for ~90 days (Table S10) in a stainless-steel double-dome housing with the same PAS configuration as used in the Global Atmospheric Passive Sampling (GAPS) network. The gap width between the upper and the lower domes was described previously [27]. The samplers allow for both gas-phase and particle-phase chemicals to be sampled at similar rates, thus passive sampler results are best treated as indicative of bulk air concentrations [17,20,27,28]. The average temperature and wind speed during the deployment period were 23 °C ± 4.1 °C and 1.9 m s^{-1} ± 0.7 m s^{-1} respectively.

Prior to their placement in the selected sites, PUFs were precleaned by Soxhlet extraction (one 24 h cycle with acetone and one 24 h cycle with hexane, both chemicals supplied by Merck, Germany). Then, PUFs were dried in desiccators for ~24 h and stored in 1 L solvent-rinsed amber glass jars for shipping. At each site, samplers were deployed approximately 5 m above the ground, inside a solvent-rinsed stainless-steel chamber [19], and assembled at the deployment site to avoid contamination. Stainless steel chambers were designed to protect the disks from sunlight, precipitation and coarse particle deposition. Field blanks (n = 4) were collected by following the same steps as for the air samples but without deployment. After collection, the PUFs were placed in solvent-rinsed aluminum foil inside polyethylene zip bags and stored in the freezer prior to extraction.

2.2.2. Sample analysis

PUFs disks were spiked with 150 μL of internal standards (IS) (PCB-143, BDE-77 and ^{13}C-BDE-209 at 100, 10 and 50 pg μL^{-1}, respectively). The PCB standard was obtained from Dr. Ehrenstorfer Laboratories (Augsburg, Germany) and PBDE standard mixtures were obtained from Wellington Laboratories (Guelph, Ontario, Canada). After IS addition, samples were Soxhlet-extracted with 100 mL n-hexane:acetone (3:1, v/v) for 4 h. The remaining extract was further cleaned up on ~8 g acidified silica (H$_2$SO$_4$ 44% w/w; Merck, Germany) and 0.5 g anhydrous sodium sulfate (Merck, Germany) column. Analytes were eluted with 15 mL hexane and 10 mL dichloromethane. The eluent was further evaporated to incipient dryness under a gentle N$_2$ stream and finally reconstituted with 80 μL isooctane.

Detection and quantification of analytes were carried out by using an Agilent 6890 GC (Palo Alto, CA, USA) coupled to an Agilent 5973 MS equipped with an electron capture negative ionization (ECNI) source, and a 30 m × 0.25 mm × 0.25 μm DB-5 capillary column (J&W Scientific, Folsom, USA). The ion source, quadrupole, and interface temperatures were set at 170, 150, and 300 °C, respectively. Helium was used as carrier gas at constant flow (1.0 mL min^{-1}), with methane as moderating gas. The electron multiplier voltage was set at 2200 V. An aliquot of the extract (1 μL) was injected in solvent vent mode (vent time 1.25 min, vent flow 54.2 mL min^{-1}, split-less time 1.50 min; initial injector temperature at 92 °C, maintained for 0.03 min, then heated at 700 °C min^{-1} to 300 °C and maintained for 30 min). The temperature of the DB-5 column was programmed from 90 °C (1.25 min) to 310 °C at a rate of 10 °C min^{-1} holding for 6.75 min. Bromine isotope ions (m/z 79 and 81) were acquired in selected ion monitoring (SIM) mode for the whole run time. The analysis of BDE 209 was performed on a 15 m × 0.25 mm × 0.10 μm DB-5 capillary column. Helium was used as carrier gas at an initial flow rate of 1.0 mL min^{-1} (kept for 5 min) and then raised to 2 mL min^{-1} at 10 mL min^{-1}. The oven temperature program started from 90 °C, kept for 1.25 min, and then increased with 15 °C min-1 to 310 °C, kept for 6 min. Methane was used as moderating gas and the ion source, quadrupole, and interface temperatures were 250, 150 and 300 °C, respectively. Dwell time was set to 50 ms. The ECNI-MS was operated in SIM mode at the m/z 484.7, 486.7 and 494.7, 496.7 for BDE 209 and 13C-BDE 209, respectively. For PCBs, HCB and DDTs, the two most intense characteristic ions were monitored in specific time segments according to elution characteristics [29,30]. Typical dwell times were 20–25 ms. Identification and quantification ions for each POP and the corresponding ISs are shown in Table S9.

Quality assurance/control measures were applied to evaluate the accuracy and reliability of the measurements. Multi-level calibration curves were created for the quantification of POPs and good linearity (r^2 > 0.997) was achieved for the concentration range found in the samples. The identification of analytes was based on relative retention times to the internal standard used for quantification, ion chromatograms of the congeners under study and the intensity ratio of the ions monitored [30]. A deviation of the ion intensity ratios within 20% of the mean values of the calibration standards was considered acceptable. As a part of quality assurance, analytical blanks consisted of 4 field blanks and 7 laboratory blanks were extracted and analyzed along with exposed PUFs (samples) to assess any contamination occurring while handling the PUFs and instrumental analysis and to evaluate method accuracy. The data was blank corrected using the average concentration detected in the analytical blanks. Peaks were only integrated when the signal-to-noise (s/n) ratio was >3; otherwise, they were considered below the method detection limits (LODs). Method limits of quantification (LOQ) were calculated as 3*SD of the procedural blanks. For compounds not detected in the blanks, the LOQ was calculated based on

the signal to noise ratio of 10/1. LOQ for analyzed pollutants ranged from 1 to 1000 pg sample^{-1} for PCBs; from 20 to 230 pg sample^{-1} for DDTs; from 1 to 30 pg sample^{-1} for PBDEs, and 40 pg sample^{-1} for HCB.

The conversion of the amount of POP accumulated in the sampler to a concentration in air basis involved the derivation of effective air sample volumes. The concentration in the air of the target analytes was calculated using the amount accumulated on the PUF disk (pg sampler^{-1}) during the corresponding sampling period, divided by the effective air sample volume (V_s). V_s was estimated for each compound and sample using the template provided by the GAPS network [31], which incorporates the average temperature during the sampling period, the air-PUF partition co-efficient for each target analyte and a default air sampling rate of 4 m^3 day^{-1} [20,32]. The template considers linear and equilibrium phases for multiple chemical classes with a wide range of volatil-ities. This is relevant for more volatile compounds (e.g., HCB and lower molecular weight PCBs) that reached the equilibrium with the PUF filter during the deployment period, resulting in reduced V_s compared to less volatile compounds. Deployment times are detailed in the Supplementary material (Table S10).

2.3. WRF/CALMET/CALPUFF modeling system

The atmospheric transport of the emitted POPs was modeled in the domain of interest using the CALMET/CALPUFF model [33]. The objective of the modeling was to generate fields of atmospheric levels of the studied compounds and to contrast this information with the values of concentrations measured in the air, and therefore assessing the capacity of the model to predict the spatial distribu-tion. The model outputs describe not only the POPs air concentra-tions but also the contribution from each simulated emission source.

The system consists of a meteorological diagnostic model in three dimensions called CALMET and a transport, dispersion, deposition and chemical transformation model called CALPUFF.

CALMET is a meteorological model that produces wind and temperatures hourly fields in a three-dimensional gridded modeling domain, necessary to run CALPUFF. Likewise, it associates variable fields in two dimensions, such as mixing layer height, surface characteristics and dispersion properties.

CALPUFF is a Gaussian puff dispersion, multilayer, non-stationary and multi-component state model, which can simulate the effects of variable weather conditions in transport, trans-formation and removal of pollutants. CALPUFF performs its calcu-lations considering terrain elevations, as well as land use features on which the modeling is performed. Detailed algorithms for the different physical processes involved in the dispersion and trans-port of pollutants and details on applications of the model can be found in the literature [22,33].

The modeling domain was organized in a grid of 90 × 90 km^2, with 8100 basic horizontal grid cells of 1 km × 1 km. Because of the high-demanding computing needs of the models, only one month was chosen to perform the simulations (January 2011). This could supply an understanding of the general distribution of POPs through the entire period (December 2010/April 2011), taking into account that the months of sampling campaign belonged to the same season, and POPs should have the same behavior during that period.

For its operation the model required the following inputs:

Topography, land use and land cover: Terrain features were incorporated using data from Shuttle Radar Topography Mission (SRTM), available in a 1-arcsecond resolution (approximately 30 m) courtesy of the U.S. Geological Survey [34]. Vegetation maps of the Global Land Cover 2000 Project (GLC 2000) for South America, with a 1 km resolution and data generated by the Department of Ge-ography of the University of Maryland (UMD Global Land Cover) were used for land use and land cover features [35].

Meteorological data: The CALMET module required meteoro-logical fields on surface and height as inputs. However, only one meteorological station was available in the study area (Mendoza Airport- AERO) and one climatological station (Parque General San Martin- PARQUE), both operated by the Argentine Weather Service (Servicio Meteorológico Nacional-SMN). Temperature and wind profiles (radiosondes) are not continuously operated. Therefore, to develop the required spatial and temporal resolution, the *W*eather *R*esearch and *F*orecasting (WRF) model [36] was used to obtain 3D fields covering the modeling domain and period [37]. The proced-ure involved the use of outputs from the regional WRF model as the initial estimate for CALMET. For this purpose, an off-line prepro-cessor called CALWRF (version 1.4) was used, which initialized CALMET replacing the required hourly parameter values of the planetary boundary layer (PBL) and the surface layer of the atmo-sphere in each grid cell with those derived from WRF. Likewise, this option allowed the capture of some flow characteristics that cannot be simulated with the inclusion of observational data due to the low density of stations. An evaluation with tracers indicated that the time fields of a mesoscale model improve the performance of dispersion models at regional scales [38]. The WRF model was used and validated previously by the authors in the study area [24,39]. Table S5 of the supplementary material shows the configuration and parameters used in the implementation of the WRF model. Fig. 2 presents the wind rose obtained in the meteorological sim-ulations (left), summarizing the average winds for the modeling period. The same figure (right) presents average values of wind speed and direction from the same period but taken from the meteorological station (AERO) and the climatological station (PARQUE).

Emissions data: The modeled compounds were DDTs, HCB, PCBs and PBDEs. Emission sources within the area of interest were sur-veyed and, based on this, we prepared our own emission inventory of the modeled species, which has been previously published [6]. Total emissions data by source is shown in Table S1. Since selected pollutants are not part of the default CALPUFF library, they were included considering the two forms in which they are emitted: gas and particles. More details about how this partitioning was calcu-lated are presented in Section S1 of the Supplementary Material. Particles were modeled as particulate matter (PM) of three different aerodynamic diameters: PM10 (10 μm or less); PM2.5 (2.5 μm or less) and PM1 (1 μm or less). For each emitting source, a charac-teristic particle-gas partition [40–43] and a size distribution for the particulate fraction [44] (Table S4) was considered to divide the total emission of each compound in the emission inventory. The sources were modeled, according to their characteristics, like area or point sources.

2.4. Model validation: statistical performance analysis

Data normality was verified for both datasets, measured and simulated, by the Shapiro-Wilk test. A Kruskal-Wallis test was applied for non-parametric distributions, in order to test differ-ences between observed and simulated concentrations of POPs. For all statistical tests, the significance level adopted was 5% ($p < 0.05$). To evaluate the ability of the air quality modeling system to reproduce the observed concentrations, five statistical performance metrics were calculated for each of the four analyzed compounds: Mean bias error (MBE), Fractional Bias (FB), Normalized Mean Square Error (NMSE), Factor of two (Fa2) and Pearson correlation coefficient (r) [45]. These metrics were allowed to assess the size of the differences and the degree of correlation between predicted
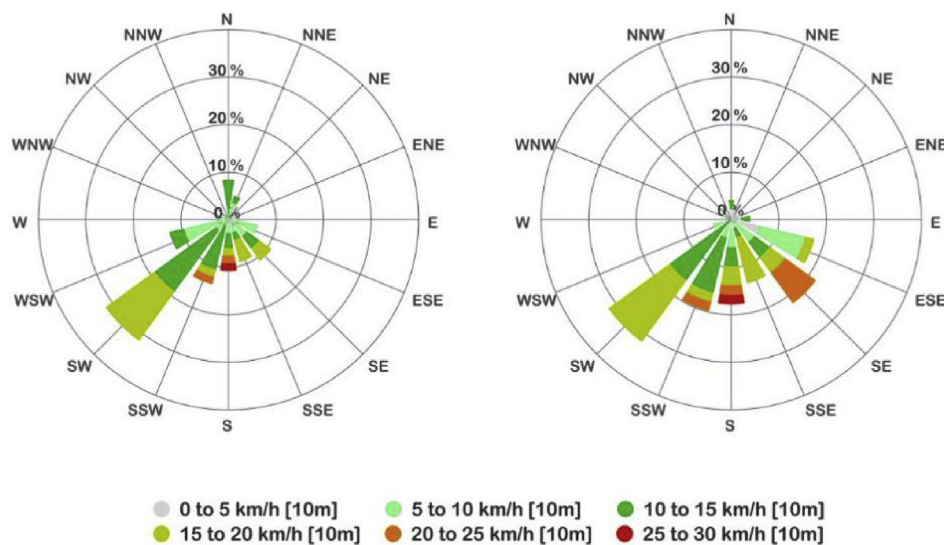
Fig. 2. Windrose constructed from simulated data (left) and from meteorological stations (right), the average for the modeled period in the study area.

and observed values. MBE is the mean error. Large overestimation or underestimation would be obscured by this measure. FB is a linear measure of bias and reflects the degree of matching between simulated and observed mean of the concentration distribution. It ranges between +2 and −2, with a perfect model resulting in FB = 0. A FB of 0.6 is equivalent to model underprediction by about a factor of two. A negative value indicates model overprediction. NMSE is a measure of variance and represents the relative scatter of the concentration distribution. A perfect model would result in an NMSE = 0, with a value of 1.0 indicating that differences between simulated values and observations are approximately equal to the mean. Fa2 reflects the percentage of predicted concentrations lying within a factor of 2 of observations. r involves statistical parameters obtained by linear least-squares regression. A value of r close to 1 indicates a perfect correlation between observed and simulated values, a sign of good model performance.

Additionally, scatter plots are presented (Fig. 3, right), to illustrate the scatter about the 1:1 (y = x) line by plotting simulated (y-axis) against the corresponding observed airborne concentrations (x-axis), which indicates a model tendency towards under/over-predictions [46].

3. Results and discussion

3.1. Air concentrations of POPs

The four POPs (namely $\sum$DDTs, HCB, $\sum$PCBs and $\sum$PBDEs) were measured in air samples at concentrations above LOQs, and their mean atmospheric levels (C_m, measured concentrations) in each sampling point are reported in Table 1.

$\sum$DDTs concentrations in air were within the range of 2.1–14.2 pg m^{-3}. In general, the highest levels were detected in samples from urban sites. This compound showed the greatest variation (SD 3.7 pg m^{-3}) among the studied POPs. These results were comparable to those reported in other studies in South America. Rauert et al. [10] found elevated DDT atmospheric concentrations in Sonora (Mexico) (8.9–95 pg m^3) and at an urban site of São Luis (Brazil) (33–78 pg m^3). At other sites in the Group of Latin America and the Caribbean (GRULAC), they measured this compound in the range of <0.7–8.3 pg m^3, comparable with the results obtained in this study. Pozo et al. [47] determined DDTs atmospheric levels in the range of 1–30 pg m^{-3} in Concepción,

Chile. In Argentina, Tombesi et al. [8] measured air concentrations of DDTs between 0.1 and 20 pg m^{-3} in different urban and agricultural sites from Bahía Blanca. Both cases [8,47] also found the highest levels in urban locations. Also in Argentina, Silva-Barni et al. [7] reported DDTs airborne concentrations between 2 and 100 pg m^{-3} in Quequén Grande River basin, located in southern Buenos Aires province, an area characterized by extensive agricultural practices.

HCB atmospheric levels showed moderated variability in the study area (SD 2.9 pg m^{-3}), being in the range of 9.2–18.5 pg m^{-3}. In this case, there was no clear spatial trend, which could be associated with the variety of emission sources of this compound (see Table S1), which could be emitted from both, agricultural and industrial activities [6]. Also, HCB presented an emissions pattern distributed uniformly throughout the study area [6]. Comparing the results obtained in this work with other studies in Latin America, HCB levels here presented were lower, especially the max values. Rauert et al. [10] measured this compound in the air of 9 sites in Latin America and Caribbean countries in 2014 and 2015. They found values ranging from 13 to 55 pg m^{-3} in 2014 and 8.8–108 pg m^{-3} in 2015. Guida et al. [15], reported HCB atmospheric levels at protected areas from Brazil between 19 and 84 pg m^{-3}, and Ornellas Meire et al. [14] also presented measurements in Brazilian air, with values from 21 to 29 pg m^{-3}.

Concentrations of ΣPCBs in the air were between 0.6 and 5.5 pg m^{-3}, showing the smallest variation among sampling sites (SD 1.8 pg m^{-3}). The highest $\sum$PCBs levels were detected at urban locations. However, the results of this study were generally lower, by a factor of 4–65, than those reported for urban areas in other Latin American cities, as Santiago de Chile (mean of 16 pg m^{-3}) [47], Bahía Blanca in Argentina (40–360 pg m^{-3}) [8] or GRULAC sites (0.08–128 pg m^3) [10]. It is important to highlight that, in general, these areas have a higher degree of industrialization compared to Mendoza, which could explain the higher levels found.

ΣPBDEs concentrations in air ranged from 0.4 to 7.6 pg m^{-3}. Similar to $\sum$PCBs, $\sum$PBDEs concentrations were higher in urban sites, in agreement with the emission sources identified previously in the study area [6]. $\sum$PBDEs levels detected in this work are similar to those reported in Argentina [11] (mean of 8.0 pg m^{-3}), Chile [47] (mean of 5.6 pg m^{-3}) and the GRULAC region [18] (ranging between 0.40 and 18 pg m^3 in 2014 and 0.86–20 pg m^3 in 2015).
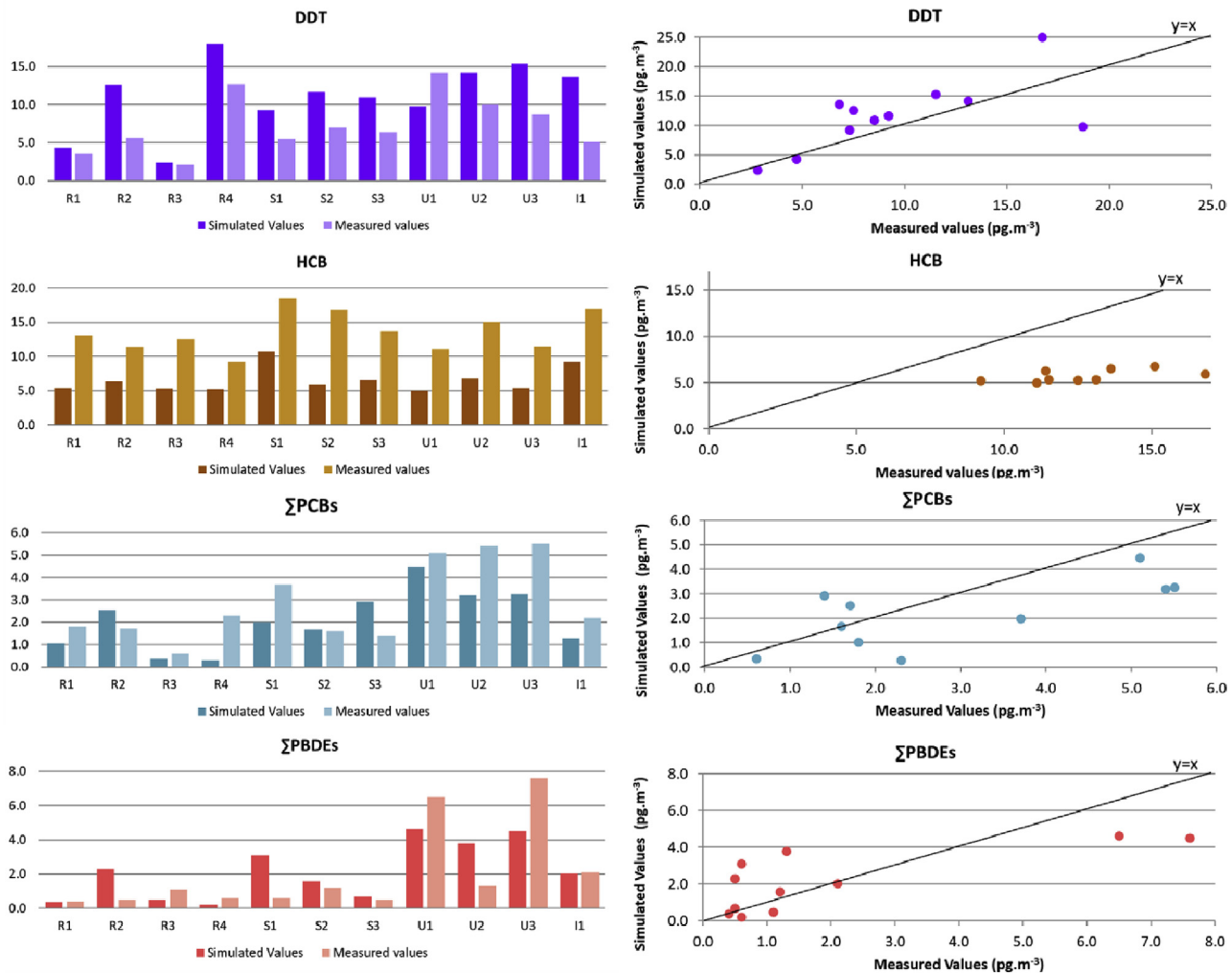
Fig. 3. Left: Comparison of measured and simulated values (pg m^{-3}) in each sampling point. Right: Scatter plots of POPs airborne concentrations (pg m^{-3}) measured vs simulated values for all the sampling points.

3.2. Validation of modeling system

In order to understand the modeling system performance, simulations were statistically compared with the observational data. Table 1 shows the atmospheric concentration values of $\sum$DDTs, HCB, $\sum$PCBs and $\sum$PBDEs (pg m^{-3}) obtained through the implementation of the model, in the sampling locations (Cs, simulated concentrations).

Data normality was verified for both datasets, observed and simulated values, by the Shapiro-Wilk test. None of the analyzed groups resulted normally distributed. Consequently, a Kruskal-Wallis test was performed, which determined that there were no statistically significant differences between the values calculated by the model and those measured in the air for $\sum$DDTs, $\sum$PCBs and $\sum$PBDEs. This result suggested a good overall performance of the applied model for these compounds. In the case of HCB, both data sets presented statistically significant differences.

Table 2 shows the performance metrics used to compare CAL-PUFF model predictions with measured concentrations for $\sum$DDTs, HCB, $\sum$PCBs and $\sum$PBDEs, following the method recommended by Kumar [45] for validation of environmental models, appropriate when the typical difference between predictions and observations are approximately a factor of two [48].

The overall results revealed good model performance in reproducing measurements at all locations, and they showed that the modeling system is suitable for the simulation of atmospheric levels of POPs in the study area. The metrics values were within the range proposed as desirable for $\sum$DDTs, $\sum$PCBs and $\sum$PBDEs, except for Fa2 for $\sum$PBDEs, which resulted in 0.64.

On the whole, $\sum$PCBs exhibited the best agreement, followed in order by $\sum$DDTs and $\sum$PBDEs. The MBE<0 and FB>0 for $\sum$PCBs means that the model tended to underestimate concentrations, which might be due to unaccounted emission sources. Another reason for this underestimation could be that modeled emissions were only those coming from primary sources, and a background level related to long-range atmospheric transport was not included. Otherwise, $\sum$DDTs and $\sum$PBDEs to a lesser extent presented MBE>0 and FB < 0, showing a tendency of the model to overestimations in these cases. NMSE and r-values further indicated that simulations reproduced measured concentrations of $\sum$DDTs, $\sum$PCBs and $\sum$PBDEs fairly well, with best NMSE of 0.25 and best r of 0.82 occurring for $\sum$DDTs.

Scatter plots (Fig. 3, right) correlating model predictions with the corresponding field determinations are presented as visual measures of performance, showing the agreement between simulated and measured values. The left column in Fig. 3 illustrates how the simulation was able in all cases to reflect the spatial pattern of

Table 1
Measured (Cm) and simulated (Cs) concentrations (pg m^{-3}) for $\sum$DDTs, HCB, $\sum$PCBs and $\sum$PBDEs at the sampling points.

	Sampling point	Location	$\sum$DDTs		HCB		$\sum$PCBs		$\sum$PBDEs	
			C_m	C_s	C_m	C_s	C_m	C_s	C_m	C_s
RURAL	R1	−32.88° −68.92°	3.5	4.3	13.1	5.4	1.8	1.0	0.4	0.4
	R2	−32.87° −68.73°	5.6	12.6	11.4	6.3	1.7	2.5	0.5	2.3
	R3	−33.09° −68.75°	2.1	2.4	12.5	5.3	0.6	0.4	1.1	0.5
	R4	−33,19° −68.93°	12.7	25.1	9.2	5.2	2.3	0.4	0.6	0.2
SUBURBAN	S1	−32.90° −68.87°	5.5	9.3	18.5	10.7	3.7	2.0	0.6	3.1
	S2	−32.96° −68.79°	7.0	11.7	16.8	5.9	1.6	1.7	1.2	1.6
	S3	−33.04° −68.88°	6.4	10.9	13.6	6.5	1.4	2.9	0.5	0.6
URBAN	U1	−32.92° −68.85°	14.2	9.8	11.1	5.0	5.1	4.5	6.5	4.6
	U2	−32.89° −68.80°	10.0	14.2	15.1	6.8	5.4	3.2	1.3	3.8
	U3	−32.92° −68.82°	8.7	15.4	11.5	5.4	5.5	3.3	7.6	4.5
INDUSTRIAL	I1	−32.94° −68.75°	5.1	13.6	17.0	9.2	2.2	1.3	2.1	2.0
Mean			7.3	11.7	13.6	6.5	2.8	2.1	2.0	2.2
Median			6.4	11.7	13.1	5.9	2.2	2.0	1.1	2.0
SD			3.7	6.0	2.9	1.8	1.8	1.3	2.5	1.7

Table 2
Statistical metrics calculated in order to evaluate the model performance.

Statistical metric	Desirable value	$\sum$DDTs	HCB	$\sum$PCBs	$\sum$PBDEs
MBE	Not defined	3.75	−7.1	−0.44	0.11
FB	$-0.5 \leq FB \leq +0.5$	−0.38	0.7	0.3	−0.05
NMSE	≤ 0.5	0.25	0.58	0.26	0.37
Fa2	≥ 0.80	0.82	0.36	0.82	0.64
r	-1	0.74	0.8	0.71	0.74

the observations, following the profile showed by these data, in terms of the increase/decrease of levels when comparing one site with another.

The metric values calculated for HCB resulted outside the desired range, showing a tendency of the model to underestimate the measured concentrations (FB = 0.7 and NMSE = 0.58). However, the r-value for this compound resulted in 0.8, suggesting a good fit for the modeled values regarding the spatial trend and variability of the measured data. This can be corroborated by observing the Fig. 3 (left), where it is shown that the spatial variations were captured by the model quite accurately, despite the underestimation reflected in Fig. 3 (right). Most likely, this may be due to an underestimation in the magnitude of the emissions, but not in their location and dispersion. It is important to highlight that the model was based on the emission inventory previously elaborated by the authors, and the model implementation is the only way to validate this inventory. As was detailed [6], the inventory was subject to its own uncertainty, which was quantified as the probability that the emissions were lower or greater than those estimated as average, generating a "distribution of probable emissions". Considering the obtained results, it could be expected that using higher probable emissions, the model would generate values of simulated concentrations closer to those measured, without affecting the pattern of spatial distribution, which, as already mentioned, was very well represented. Nevertheless, adjustments in the emission inventory exceed the aim of this work.

3.3. Spatial distribution of POPs in the atmosphere of the study area

The concentration maps generated by the model (Fig. 4) showed a marked horizontal gradient, with the highest concentrations located around the emission sources. Terrain features, especially the presence of the mountain range to the west, together with the prevailing wind direction produced a pollutant dispersion towards the northeast.

Modeled concentrations showed good agreement with the emission inventory and land use features. For HCB and $\sum$DDTs, which are used as part of the formulation of agrochemicals, the dispersion pattern reached greater spatial distribution due to the large proportion of the study area that reports agricultural activity. On the other hand, $\sum$PCBs and $\sum$PBDEs showed higher maximum levels, in accordance with the emissions inventory. These hotspots were located around the main emission sources, especially those sites where the open burning of MSW takes place. Because the emission sources of $\sum$PCBs and $\sum$PBDEs presented a more limited spatial distribution, the minimum levels of these substances were also lower than for $\sum$DDTs and HCB.

It is noteworthy that the lowest or highest levels predicted by the model occurred in areas where no samples were taken, which means that the set of measured data, by themselves, may not have correctly reflected the concentrations range in the study area. Fig. 5 exhibits the distribution of POPs airborne concentrations obtained from measured and simulated data, in logarithmic scale for better visualization. Boxes corresponding to measured data were made from collected samples (n = 11), while boxes representing simulated data were prepared from the complete output data of the model, which included 8100 values, in the center of each cell that formed the modeling grid. This boxplot shows that, even when measured data was able to represent the average POPs air concentrations in the study area, the allocation of the samplers did not allow to reflect the real spatial gradient of POPs levels, since boxes of simulated concentrations shows that spatial variability would be much greater, towards both lowest and highest values.
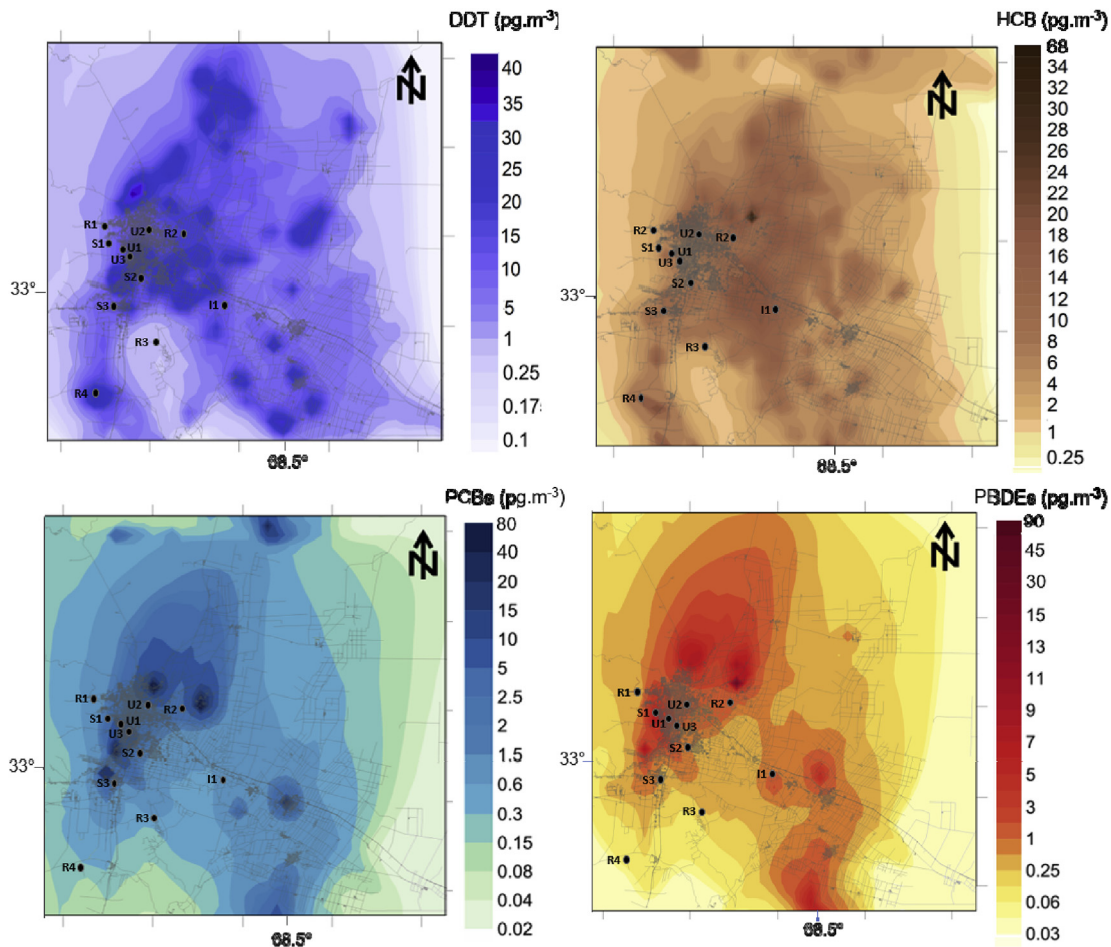
Fig. 4. Modeled 1-month average POPs airborne concentrations (pg m^{-3}) in the study area.
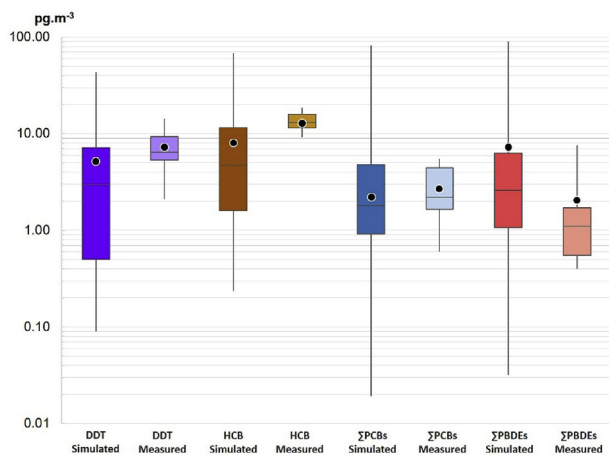

Fig. 5. Box and whisker plots showing the distribution of measured and simulated POPs airborne concentrations (pg m^{-3}) in the study area. The bottom and top of the box are the first and third quartiles, the band inside the box is the second quartile (median). The ends of the whiskers represent the minimum and maximum values, and black dots are mean values.

3.4. Source apportionment

The implementation of the model allowed an analysis of the relative contribution of modeled sources to air quality in the study area, which is especially important to make decisions and to implement policies regarding the emissions ban/reduction.

At the sampling sites, source apportionment was conducted to assess the contribution of each source category to airborne concentrations. In the interest of this work, sources were categorized according to the emission inventory [6], based on the Stockholm Convention, Annex C, Parts II and III [1]. ∑DDTs were not considered in this analysis since it was determined that the only emission source is the application of pesticides.

Tables S6–S8 summarize the contribution of modeled sources to POPs airborne concentration at the eleven sampling locations, both in percentages and concentrations. Results (Fig. 6) indicated the prevalence of emissions from open burning of MSW (ranging from 9% to 90%) on the simulated POPs concentrations. HCB presented the lowest mean proportion coming from this activity (37%) but the highest variability (SD = 20%). PCBs had a contribution from this source of 69 ± 9%, and the PBDEs showed the highest percentages and the lowest variability (84 ± 4%).

HCB showed the greatest difference in the profile of the contribution of each site. For this compound, a clear spatial pattern was not evidenced regarding the total levels, but it could be noticed in the contributions by source, where the rural locations presented greater contribution from the application of pesticides, followed by suburban locations and finally by urban and industrial sites, where the highest percentage was contributed by open burning of MSW.

For PCBs, the open burning of MSW was the emission source that contributed most to simulated levels in all the studied sites,
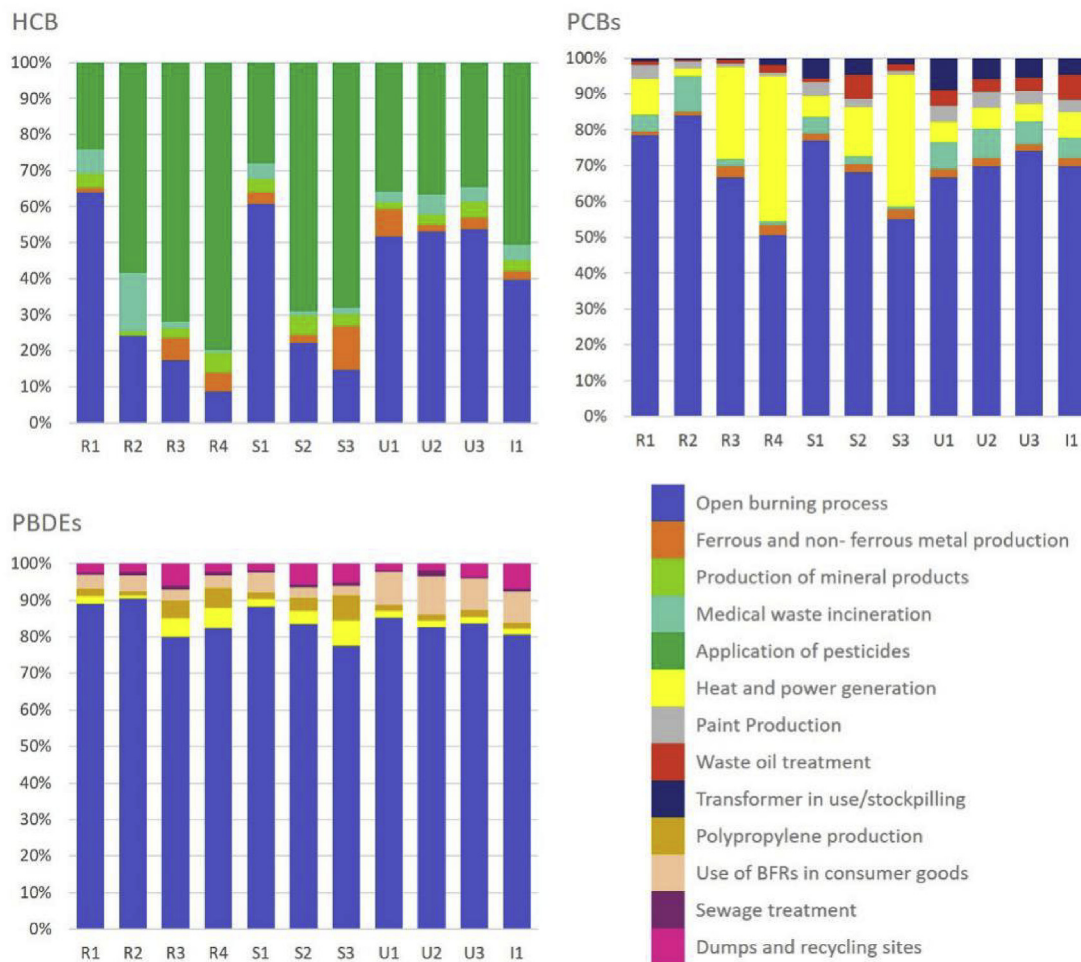
Fig. 6. Percentage contribution by source to the total atmospheric levels of POPs at the sampling points.

exceeding 50% of the total in all cases. This pollutant also presented the greatest contribution from industrial sources, especially from the heat and power generation industry, with an average of 14%, reaching up to 40% at sites closer to this facility. Emissions from stockpiling and use of transformers represented a very low proportion of total emissions, less than 1%, but their contribution to simulated levels in the sites closer to the emission zones (U1, U2, U3, I1) was considerable, in a range between 5% and 9%. In the case of the emissions produced by treatment of waste oils, the situation was similar, since points located in the vicinity of the treatment plant (S2 and I1) presented contributions from this activity of 7%.

∑PBDEs presented the contribution pattern most uniform among the studied POPs. The open burning of MSW represented the largest contribution at all sites, in a range from 79% to 90%. Use of FRs in consumer goods had more relevance in urban locations, reaching 10% in U2. Sites located to the south of the study area (R3, R4, S3) presented greater contribution from the generation of heat and energy and production of polypropylene industries, due to the proximity to the plants.

4. Conclusion

In this work, an assessment of the spatial distribution, patterns and source contributions of POPs in the atmosphere of Great Mendoza, Argentina, was carried out. The WRF/CALMET/CALPUFF modeling system was used to simulate POPs airborne

concentrations in the study area, where different atmospheric POPs sources are located. Analytical determinations in air samples collected using passive samplers were also carried out in order to validate the model.

Statistical analysis was executed, comparing modeled atmospheric POPs concentrations against airborne concentrations analytically determined. It showed a satisfactory agreement in the study area. Therefore, the modeling system could be used to predict POPs airborne concentrations with reasonable accuracy at a local scale.

Model output was used to examine the relative source contribution to ground-level concentrations in air, and to assess the spatial variability of the studied POPs. Source apportionment revealed the prevalence of emissions from open burning of municipal solid waste (ranging from 9% to 90%) on the simulated POPs concentrations, excepted for ∑DDTs, where the application of pesticides was the only emission source.

The spatial pattern obtained from simulations exhibited that the lowest or highest levels predicted by the model occurred in areas where no samples were taken, suggesting that the real gradient in the POPs air concentrations would be much greater. In this sense, it is noteworthy the usefulness of the implementation of an atmospheric dispersion model, not only in the study of air quality and exposure levels, but also as a tool for the proper design of monitoring networks, taking into account the time and cost that sampling campaigns take, and the conclusions that are intended to be made from the analysis of the obtained data.

Declaration of competing interest

Each named author has substantially contributed to conducting the underlying this research and drafting the uploaded manuscript. The named authors declare that they have no conflict of interest, financial or otherwise related with this investigation and the content presented in the manuscript.

Acknowledgment

Appendix A. Supplementary data

Supplementary data to this article can be found online at https://doi.org/10.1016/j.emcon.2020.02.002.

References

[1] UNEP, Stockholm Convention on Persistent Organic Pollutants, POPs, Stockholm, Sweden, 2009.

[2] Economic Commission for Latin America and the Caribbean, Observatory on Principle 10 in Latin America and the Caribbean [Internet], Stock. Conv. Persistent Org. Pollut, 2016. Available from: https://observatoriop10.cepal.org/en/treaties/stockholm-convention-persistent-organic-pollutants.

[3] SAyDS, Ley 26.011: Aprobación del Convenio de Estocolmo sobre Contaminantes Orgánicos Persistentes [Internet], 2005. Available from: http://servicios.infoleg.gob.ar/infolegInternet/anexos/100000-104999/102996/norma.htm.

[4] SAGyP, Decreto 2121/90: Prohibición de importación, fabricación, fraccionamiento, comercialización y uso de productos de aplicación agrícola formulados a base de determinados principios activos, 1990.

[5] SAyDS, Ley 25.670: PCBs: Presupuestos para su gestión y eliminación [Internet], 2002. Available from: http://servicios.infoleg.gob.ar/infolegInternet/verNorma.do?id=79677.

[6] D. Allende, M.F. Ruggeri, B. Lana, K. Garro, J. Altamirano, E. Puliafito, Inventory of primary emissions of selected persistent organic pollutants to the atmosphere in the area of Great Mendoza, Emerg. Contam. 2 (2016) 14—25.

[7] M.F. Silva-Barni, M. Gonzalez, F. Wania, Y.D. Lei, K.S.B. Miglioranza, Spatial and temporal distribution of pesticides and PCBs in the atmosphere using XAD-resin based passive samplers: a case study in the Quequén Grande River watershed, Argentina [Internet]. Elsevier B.V. Atmos. Pollut. Res. 9 (2018) 238—245, https://doi.org/10.1016/j.apr.2017.09.008. Available from:

[8] N. Tombesi, K. Pozo, T. Harner, Persistent Organic Pollutants (POPs) in the atmosphere of agricultural and urban areas in the Province of Buenos Aires in Argentina using PUF disk passive air samplers [Internet]. Elsevier, Atmos. Pollut. Res. 5 (2014), 170—8. Available from: http://www.atmospolres.com/articles/Volume5/issue2/APR-14-021.pdf.

[9] M.J. Astoviza, N. Cappelletti, C. Bilos, M.C. Migoya, J.C. Colombo, Airborne PCB patterns and urban scale in the Southern Río de la Plata Basin, Argentina [Internet]. Elsevier B.V. Sci. Total Environ. 572 (2016) 16—22, https://doi.org/10.1016/j.scitotenv.2016.07.101. Available from:

[10] C. Rauert, T. Harner, J.K. Schuster, A. Eng, G. Fillmann, L.E. Castillo, et al., Air monitoring of new and legacy POPs in the Group of Latin America and Caribbean (GRULAC) region [Internet]. Elsevier Ltd, Environ. Pollut. 243 (2018) 1252—1262, https://doi.org/10.1016/j.envpol.2018.09.048. Available from:.

[11] K. Pozo, T. Harner, S.C. Lee, F. Wania, D.C.G. Muir, K.C. Jones, Seasonally resolved concentrations of persistent organic pollutants in the global atmosphere from the first year of the GAPS Study, Environ. Sci. Technol. 43 (2009) 796—803.

[12] C.N. Pegoraro, T. Harner, K. Su, M.S. Chiappero, Assessing levels of POPs in air over the south atlantic ocean off the coast of south America, Sci. Total Environ. 571 (2016) 172—177.

[13] C. Rauert, J.K. Schuster, A. Eng, T. Harner, Global atmospheric concentrations of brominated and chlorinated flame retardants and organophosphate esters, Environ. Sci. Technol. 52 (2018) 2777—2789.

[14] R. Ornellas Meire, M. Khairy, A.C. Targino, P.M.A. Galvão, J.P.M. Torres, O. Malm, et al., Use of passive samplers to detect organochlorine pesticides in air and water at wetland mountain region sites (S-SE Brazil), Chemosphere 144 (2016) 2175—2182.

[15] Y. de S. Guida, R.O. Meire, J.P.M. Torres, O. Malm, Air contamination by legacy and current-use pesticides in Brazilian mountains: an overview of national regulations by monitoring pollutant presence in pristine areas, Environ. Pollut. 242 (2018) 19—30.

[16] A. De la Torre, P. Sanz, I. Navarro, M.Á. Martínez, Time trends of persistent organic pollutants in Spanish air, Environ. Pollut. 217 (2016) 26—32.

[17] A. Saini, J. Clarke, N. Jariyasopit, C. Rauert, J.K. Schuster, S. Halappanavar, et al., Flame retardants in urban air: a case study in Toronto targeting distinct source sectors [Internet]. Elsevier Ltd, Environ. Pollut. 247 (2019) 89—97, https://doi.org/10.1016/j.envpol.2019.01.027. Available from:.

[18] C. Rauert, T. Harner, J.K. Schuster, A. Eng, G. Fillmann, L.E. Castillo, et al., Atmospheric concentrations of new persistent organic pollutants and emerging chemicals of concern in the group of Latin America and caribbean (GRULAC) region, Environ. Sci. Technol. 52 (2018) 7240—7249.

[19] L. Melymuk, M. Robson, P.a. Helm, M.L. Diamond, Evaluation of passive air sampler calibrations: selection of sampling rates and implications for the measurement of persistent organic pollutants in air [Internet]. Elsevier Ltd, Atmos. Environ. 45 (2011) 1867—1875, https://doi.org/10.1016/j.atmosenv.2011.01.011. Available from:.

[20] T. Harner, J.K. Schuster, E. Sverko, L.M. Jantunen, S.C. Lee, K. Pozo, Surveillance of new priority chemicals in air under the global atmospheric passive sampling (gaps) network, Organohalogen Compd. 76 (2014) 1309—1312.

[21] J. Duyzer, D. van den Hout, P. Zandveld, S. van Ratingen, Representativeness of air quality monitoring networks [Internet]. Elsevier Ltd, Atmos. Environ. 104 (2015) 88—101, https://doi.org/10.1016/j.atmosenv.2014.12.067. Available from:.

[22] B. Harnett, T. Hawes, T. Allen, Technical Issues Related to Use of the CALPUFF Modeling System for Near-Field Applications, 2008. Research Triangle Park.

[23] J. Michalakes, J. Dudhia, D. Gill, T. Henderson, J. Klemp, W. Skamarock, et al., The weather research and forecast model: software architecture and performance, in: Use High Perform Comput Meteorol - Elev ECMWF Work. United Kingdom, 2004, pp. 156—168.

[24] S.E. Puliafito, D.G. Allende, C.G. Mulena, P. Cremades, S.G. Lakkis, Evaluation of the WRF model configuration for zonda wind events in a complex terrain, Atmos. Res. 166 (2015) 24—32.

[25] U. Schlink, O. Herbarth, M. Richter, M. Rehwagen, J.L. Puliafito, S.E. Puliafito, et al. [Internet], Ozone-monitoring in Mendoza, Argentina : Initial Results. J Air Waste Manage Assoc, vol. 49, Air & Waste Management Association, 1999, 82—7. Available from: http://cat.inist.fr/?aModele=afficheN&cpsidt=1635658.

[26] C. Chaemfa, J.L. Barber, K.S. Kim, T. Harner, K.C. Jones, Further studies on the uptake of persistent organic pollutants (POPs) by polyurethane foam disk passive air samplers [Internet]. Elsevier Ltd, Atmos. Environ. 43 (2009) 3843—3849, https://doi.org/10.1016/j.atmosenv.2009.05.020. Available from:.

[27] M.Z. Markovic, S. Prokop, R.M. Staebler, J. Liggio, T. Harner, Evaluation of the particle infiltration efficiency of three passive samplers and the PS-1 active air sampler [Internet]. Elsevier Ltd, Atmos. Environ. 112 (2015) 289—293, https://doi.org/10.1016/j.atmosenv.2015.04.051. Available from:.

[28] L. Melymuk, M. Robson, P.A. Helm, M.L. Diamond, PCBs, PBDEs, and PAHs in Toronto air: spatial and seasonal trends and implications for contaminant transport [Internet]. Elsevier B.V. Sci. Total Environ. 429 (2012) 272—280, https://doi.org/10.1016/j.scitotenv.2012.04.022. Available from:

[29] N. Ali, R.N. Malik, T. Mehdi, S.A.M.A.S. Eqani, A. Javeed, H. Neels, et al., Organohalogenated contaminants (OHCs) in the serum and hair of pet cats and dogs: biosentinels of indoor pollution [Internet]. Elsevier B.V. Sci. Total Environ. 449 (2013) 29—36, https://doi.org/10.1016/j.scitotenv.2013.01.037. Available from:

[30] V.L.B. Jaspers, C. Sonne, F. Soler-Rodriguez, D. Boertmann, R. Dietz, M. Eens, et al., Persistent organic pollutants and methoxylated polybrominated diphenyl ethers in different tissues of white-tailed eagles (Haliaeetus albicilla) from West Greenland [Internet]. Elsevier Ltd, Environ. Pollut. 175 (2013) 137—146, https://doi.org/10.1016/j.envpol.2012.12.023. Available from:.

[31] T. Harner, Template for Calculating Effective Air Sample Volumes for PUF and SIP Disk Samplers [Internet], 2017. Available from: https://www.researchgate.net/publication/319764519_2017_v1_5_Template_for_calculating_Effective_Air_Sample_Volumes_for_PUF_and_SIP_Disk_Samplers_Sept_15.

[32] K. Pozo, T. Harner, M. Shoeib, R. Urrutia, R. Barra, O. Parra, et al., Passive-sampler derived air concentrations of persistent organic pollutants on a north-south transect in Chile, Environ. Sci. Technol. 38 (2004) 6529—6537.

[33] J.S. Scire, D.G. Strimaitis, R.J. Yamartino, A User ' S Guide for the CALPUFF Dispersion Model. Control, 2000.

[34] U.S. Geological Survey, Earth explorer [Internet], Available from: https://earthexplorer.usgs.gov/, 2017.

[35] M. Hansen, R. DeFries, J.R.G. Townshend, R. Sohlberg, UMD Global Land Cover Classification, 1 Kilometer, 1.0e, 1998. College Park, Maryland.

[36] W.C. Skamarock, J.B. Klemp, D.O. Gill, D.M. Barker, W. Wang, J.G. Powers, A description of the advanced research WRF version 3, NCAR Techical Notes (2008). https://opensky.ucar.edu/islandora/object/technotes%3A500/datastream/PDF/view.

[37] J.S. Scire, F.R. Robe, M.E. Fernau, R.J. Yamartino, A User's Guide for the CALMET Meteorological Model (Version 5), Earth Tech Inc., 2000. http://www.src.com/calpuff/download/CALMET_UsersGuide.pdf.

[38] U.S Environmental Protection Agency, Testing of Meteorological and Dispersion Models for Use in Regional Air Quality Modeling, National Service Center for Environmental Publications (NSCEP), 1995.

[39] G.C. Mulena, D.G. Allende, S.E. Puliafito, S.G. Lakkis, P.G. Cremades, A.G. Ulke,

Examining the influence of meteorological simulations forced by different initial and boundary conditions in volcanic ash dispersion modelling, Atmos. Res. 176−177 (2016) 29−42, https://doi.org/10.1016/j.atmosres.2016.02.009.

[40] L.G. Chen, B.X. Mai, X.H. Bi, S.J. Chen, X.M. Wang, Y. Ran, et al., Concentration levels, compositional profiles, and gas-particle partitioning of polybrominated diphenyl ethers in the atmosphere of an urban city in South China, Environ. Sci. Technol. 40 (2006) 1190−1196.

[41] C. Degrendele, K. Okonski, L. Melymuk, L. Landlová, P. Kukučka, O. Audy, et al., Pesticides in the atmosphere: a comparison of gas-particle partitioning and particle size distribution of legacy and current-use pesticides [Internet], Atmos. Chem. Phys. Discuss. 15 (2015) 23651−23681. Available from: http://www.atmos-chem-phys-discuss.net/15/23651/2015/.

[42] M. Mandalakis, M. Tsapakis, A. Tsoga, E.G. Stephanou, Gas-particle concentrations and distribution of aliphatic hydrocarbons, PAHs, PCBs and PCDD/Fs in the atmosphere of Athens (Greece), Atmos. Environ. 36 (2002) 4023−4035.

[43] M.F. Simcik, T.P. Franz, H. Zhang, S.J. Eisenreich, Gas-particle partitioning of PCBs and PAHs in the Chicago urban and adjacent coastal atmosphere: States of equilibrium, Environ. Sci. Technol. 32 (1998) 251−257.

[44] U.S Environmental Protection Agency, Appendix B.2 Generalized Particle Size Distributions. Compil Air Pollut Emiss Factors, Vol I Station Point Area Sources, AP-42, vol. 90, 1995, pp. 1−22.

[45] A. Kumar, S. Dixit, C. Varadarajan, A. Vijayan, A. Masuraha, Evaluation of the AERMOD dispersion model as a function of atmospheric stability for an urban area, Environ. Prog. 25 (2006) 141−151.

[46] K. Ghannam, M. El-Fadel, A framework for emissions source apportionment in industrial areas: MM5/CALPUFF in a near-field application, J. Air Waste Manag. Assoc. 63 (2013) 190−204.

[47] K. Pozo, G. Oyola, V.H. Estellano, T. Harner, A. Rudolph, P. Prybilova, et al., Organic Pollutants (POPs) in the atmosphere of three Chilean cities using passive air samplers [Internet]. Elsevier B.V. Sci. Total Environ. (2016) https://doi.org/10.1016/j.scitotenv.2016.11.054. Available from:

[48] A.S. Rood, Performance evaluation of AERMOD, CALPUFF, and legacy air dispersion models using the Winter Validation Tracer Study dataset [Internet]. Elsevier Ltd, Atmos. Environ. 89 (2014) 707−720, https://doi.org/10.1016/j.atmosenv.2014.02.054. Available from:.